A CHORD DIAGRAM OF A RIBBON SURFACE-LINK

Akio Kawauchi

Osaka City University Advanced Mathematical Institute

Sugimoto, Sumiyoshi-ku, Osaka 558-8585, Japan

kawauchi@sci.osaka-cu.ac.jp

ABSTRACT

A ribbon chord diagram, or simply a chord diagram, of a ribbon surface-link in the 4-space is introduced. Links, virtual links and welded virtual links can be described naturally by chord diagrams with the corresponding moves, respectively. Some moves on chord diagrams are introduces by overseeing these special moves. Then the faithful equivalence on ribbon surface-links is stated in terms of the moves on chord diagrams. This answers questions by Y. Nakanishi and Y. Marumoto affirmatively. The faithful TOP-equivalence on ribbon surface-links derives the same result. By combining a previous result on TOP-triviality of a surface-knot, a ribbon surface-knot is DIFF-trivial if and only if the fundamental group is an infinite cyclic group. This corrects an erroneous proof in T. Yanagawa's old paper.

Keywords: Chord diagram, Ribbon surface-link, Virtual link, Reidemeister move, Chord diagram move, Smooth unknotting.

Mathematics Subject Classification 2010: 57Q45, 57M25, 57M05

1. Introduction

A ribbon surface-link in the 4-space $\mathbf{R}^4$ defined in [16] is described as a ribbon chord diagram, or simply a chord diagram in Section 2, which is a diagram of a chord graph, a trivalent spatial graph in the 3-space $\mathbf{R}^3$ consisting of a trivial link called based loops and arcs called chords.[1] We investigate a transformation from a link diagram or a virtual link diagram to a chord diagram of a ribbon torus-link which is defined by observing Artin's spinning construction [1] for a classical link

[1] Our basic techniques depend on the papers [15, 16]. Earlier arguments in T. Yajima's papers [23, 24] and T. Yanagawa's paper [26] are also helpful here.

and by observing Satoh's construction [21] for a virtual or welded virtual link. In this section, we also investigate consequences of the classical, virtual and welded virtual Reidemeister moves to chord diagrams. In Section 3, three kinds of moves on the chord diagrams, called M_0, M_1 and M_2 are introduced as moves relaxing the classical, virtual and welded virtual Reidemeister moves given in Section 2. The move M_0 is nothing but the Reidemeister moves on diagrams of trivalent spatial graphs. The move M_1 is a move on the based loops, called the fusion-fission move, which is equivalent under the use of the move M_0 to the elementary fusion-fission move $M_{1.0}$, the moves of the chord slide $M_{1.1}$ and the chord pass $M_{1.2}$. In Section 4, first of all, the definition of a faithful equivalence on ribbon surface-links is made as an equivalence together with a homotopical vanishing condition on meridians of the ribbon 1-handles. Then the main result (Theorem 4.1) saying that two ribbon surface-links are faithfully equivalent if and only if any chord diagrams of them are mutually deformed into each other by a finite number of the moves M_0, M_1 and M_2 is stated and proved. This answers questions by Y. Nakanishi in [19] and Y. Marumoto in [17] affirmatively. A main idea of this proof is outlined as follows: Given a faithful equivalence on ribbon surface-links F and F', then we send a chord graph put on F to F' by the faithful equivalence. Then we deform the image of the chord graph into a chord graph of F' put on F' homotopically while using the moves M_0, M_1 and M_2 on the chord diagrams. In Section 5, it is observed in Corollary 5.1 that the topological version of Theorem 4.1 holds without essential change. This means that any two ribbon surface-links are faithfully TOP-equivalent if and only if they are faithfully equivalent. A surface-knot F in $\mathbf{R}^4$ is *DIFF-trivial* or *TOP-trivial* respectively if F bounds a handlebody embedded in $\mathbf{R}^4$ by a smooth embedding or a locally-flat topological embedding. It is proved in [4] and [13] that a surface-knot F in $\mathbf{R}^4$ is TOP-trivial if and only if the fundamental group $\pi_1(\mathbf{R}^4 \setminus F)$ is an infinite cyclic group. As a consequence of Corollary 5.1, we see that a ribbon surface-knot F is DIFF-trivial if and only if the fundamental group $\pi_1(\mathbf{R}^4 \setminus F)$ is an infinite cyclic group (Corollary 5.3). This corrects an erroneous proof of T. Yanagawa's old paper [27].

The author would like to thank Seiichi Kamada and Shin Satoh for helpful comments for this research. An essential part of this paper is completed during his stay at the Chinese University of Hong Kong, where he thanks Zhongtao Wu for his nice hospitalities.

2. A ribbon surface-link and a ribbon chord diagram

A *band surgery* on an oriented link ℓ in $\mathbf{R}^3$ is a transformation of ℓ into an oriented link ℓ' by a band b spanning ℓ such that $\ell' = \mathrm{cl}(\ell \setminus \ell \cap b) \cup \mathrm{cl}(\partial b \setminus \ell \cap b)$ (see Fig. 1).

For the real line $\mathbf{R}$, the 4-space $\mathbf{R}^4$ is considered as

$$\mathbf{R}^4 = \{(x,t) |\, x \in \mathbf{R}^3, t \in \mathbf{R}\}.$$

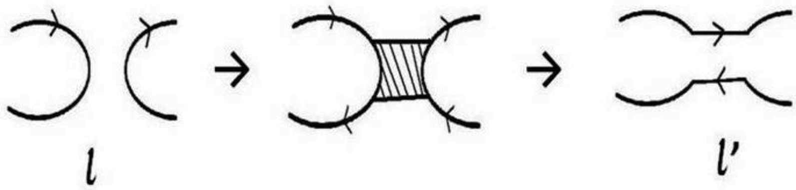

Figure 1: A band surgery

For an interval $[a,b]$ and a subset $A \subset \mathbf{R}^3$, we use the notation

$$A[a,b] = \{(x,t)|\, x \in A, t \in [a,b]\}.$$

The *realizing surface* of a band surgery $\ell \to \ell'$ on finitely many mutually disjoint bands β_j $(j = 1, 2, \dots, p)$ is a surface F_a^b in $\mathbf{R}^3[a,b]$ defined by the following identity:

$$F_a^b \cap \mathbf{R}^3[t] = \begin{cases} \ell'[t] & (\frac{a+b}{2} < t \leqq b) \\ (\ell \cup b_1 \cup \cdots \cup b_p)[t] & (t = \frac{a+b}{2}) \\ \ell[t] & (a \leqq t < \frac{a+b}{2}) \end{cases}$$

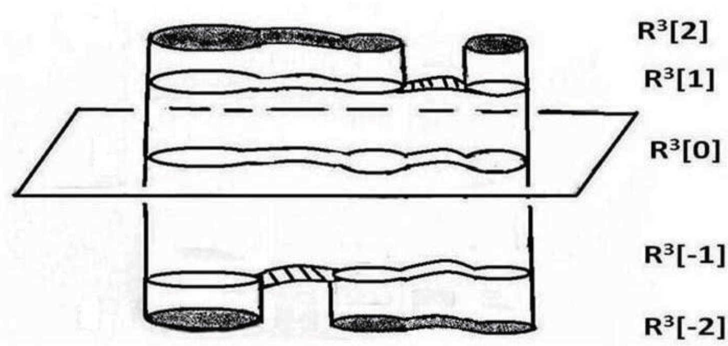

Figure 2: A closed realizing surface $\hat{F}_{-2}^{2}$ in $\mathbf{R}^3[-2,2]$

For a band surgery sequence $\ell_0 \to \ell_1 \to \cdots \to \ell_m$ and an increasing real sequence $a = a_0 < a_1 < \cdots < a_m = b$, we can construct the realizing surface

$$F_a^b = F_{a_0}^{a_1} \cup F_{a_1}^{a_2} \cup \cdots \cup F_{a_{m-1}}^{a_m}$$

of the band surgery sequence $\ell_0 \to \ell_1 \to \cdots \to \ell_m$ in $\mathbf{R}^3[a,b]$, whose topological type is independent of particular choices of the numbers $a_i\,(i = 1, 2, \dots, m-1)$. If the links ℓ_0 and ℓ_m are trivial, then we have disk systems d and d' in $\mathbf{R}^3$ bounded by ℓ_0 and ℓ_m, respectively, so that we can construct a closed oriented surface

$$\hat{F}_a^b = d[a] \cup F_a^b \cup d'[b]$$

in $\mathbf{R}^3[a,b]$, which we call the *closed realizing surface* of the band surgery sequence $\ell_0 \to \ell_1 \to \cdots \to \ell_m$ in $\mathbf{R}^3[a,b]$ (see Fig. 2).

A *surface-link* in $\mathbf{R}^4$ is a closed oriented (possibly disconnected) surface F embedded in $\mathbf{R}^4$ by a smooth embedding or a piecewise-linear locally flat embedding. When F is connected, it is called a *surface-knot* in $\mathbf{R}^4$. Two surface-links F and F' in $\mathbf{R}^4$ are *equivalent* if there is an orientation-preserving smooth or piecewise-linear homeomorphism $f : \mathbf{R}^4 \to \mathbf{R}^4$ sending F to F' orientation-preservingly. The following lemma called *Horibe-Yanagawa's lemma* is shown in [15].

Lemma 2.1. Any two closed realizing surfaces constructed from the same realizing surface F_a^b by using any disk systems are equivalent by an equivalence $f : \mathbf{R}^4 \to \mathbf{R}^4$ keeping $\mathbf{R}^3[a+\varepsilon, b-\varepsilon']$ fixed for any sufficiently small positive numbers $\varepsilon, \varepsilon'$.

We use the following definition of a ribbon surface-link given in [16]:

Definition. A surface-link F in $\mathbf{R}^4$ is *ribbon* if F is equivalent to the closed realizing surface of a band surgery sequence

$$o \to \ell \to o$$

such that o is a trivial link in $\mathbf{R}^3$ and the band surgery $\ell \to o$ is the inverse of $o \to \ell$ (see Fig. 3).

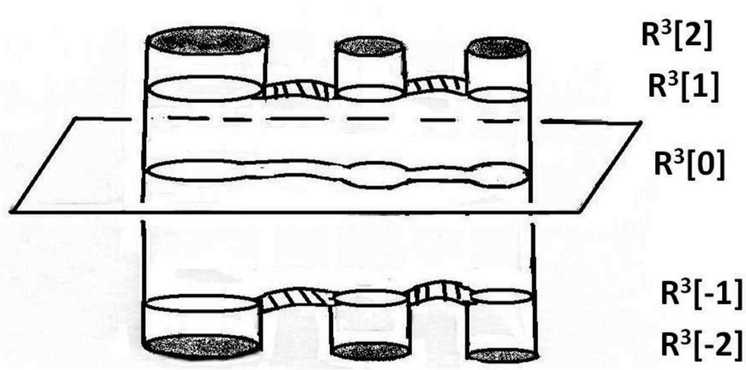

Figure 3: A ribbon surface-knot in $\mathbf{R}^3[-2,2]$

An *embedded 1-handle* on a surface-link F in $\mathbf{R}^4$ is the image $h = \mathrm{im}(\psi)$ of an embedding

$$\psi : D^2 \times I \to \mathbf{R}^4$$

such that

$$F \cap h = \psi(D^2 \times \{0,1\}),$$

where D^2 is the unit disk and $I = [0,1]$. The *surface-link obtained from F by surgery along the embedded 1-handle h* is the surface-link

$$F' = \mathrm{cl}(F \setminus F \cap h) \cup \mathrm{cl}(\partial h \setminus F \cap h)$$

in $\mathbf{R}^4$. The following characterization of a ribbon-surface-link is given in [16], which is reproved here because we use a property of this characterization.

Lemma 2.2. An oriented surface-link F in $\mathbf{R}^4$ is ribbon if and only if F is obtained from a trivial S^2-link

$$O = S_0^2 \cup S_1^2 \cup \cdots \cup S_n^2$$

in $\mathbf{R}^4$ by surgery along embedded 1-handles h_j $(j = 1, 2, \ldots, s)$ on O.

Proof of Lemma 2.2. By definition, a ribbon surface-link F is equivalent to a surface-link obtained from the trivial S^2-link

$$O = d[-2] \cup o[-2,2] \cup d[2]$$

by surgery along the 1-handles

$$(\beta_1 \cup \beta_2 \cup \cdots \cup \beta_s)[-1,1],$$

where o is a trivial link in $\mathbf{R}^3$, d is a disk system bounded by o and $\beta_j (j = 1, 2, \ldots, s)$ are the bands used for the band surgery $o \to \ell$ (see Fig. 4).

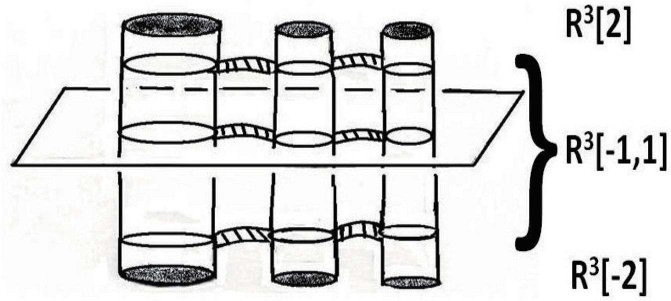

Figure 4: Creating a 1-handle from a band

Conversely, assume that F is obtained from a trivial S^2-link O by surgery along 1-handles h_j $(j = 1, 2, \ldots, s)$ on O. Let α_j be a core arc of h_j attaching to O. Let F' be another surface-link obtained from O by a surgery along 1-handles h'_j $(j = 1, 2, \ldots, s)$

on O, and α'_j a core arc of h'_j attaching to O. We use the following lemma seen from [6, Theorem 1.2]:

Lemma 2.3. If α'_j is homotopic to α_j by a homotopy relative to O in $\mathbf{R}^4$, then F' is equivalent to F.

Let $O = d[-2] \cup o[-2,2] \cup d[2]$ for a trivial link o in $\mathbf{R}^3$ and a disk system d bounded by o. Assume that the endpoints of the arcs α_j $(j = 1, 2, \ldots, s)$ are in $\mathbf{R}^3[0]$ and by a general position argument the projection images α'_j $(j = 1, 2, \ldots, s)$ of α_j $(j = 1, 2, \ldots, s)$ into $\mathbf{R}^3[0]$ are mutually disjoint embedded arcs. Then α'_j $(j = 1, 2, \ldots, s)$ are homotopic to α_j $(j = 1, 2, \ldots, s)$ by a homotopy relative to O. By Lemma 2.3, we can assume that the arcs α_j $(j = 1, 2, \ldots, s)$ are in $\mathbf{R}^3[0]$. Let β_j be a band spanning o in $\mathbf{R}^3$ such that α_j is a core arc of β_j. The surface-link F is equivalent to the surface-link obtained from O by surgery along the 1-handles $h_j = \beta_j[-1, 1]$ $(j = 1, 2, \ldots, s)$ on O. (The latter surface-link will be denoted by $\hat{F}^2_{-2}(o, \alpha)$.) Hence F is a ribbon surface-link, completing the proof of Lemma 2.2. □

By Lemmas 2.2 and 2.3, we have the following corollary.

Corollary 2.4. Every oriented ribbon surface-link is presented as a union of an oriented trivial link $o = \cup_{i=0}^{n} o_i$ and the arcs $\alpha = \cup_{j=1}^{s} \alpha_j$ spanning o in $\mathbf{R}^3$ (see Fig. 5).

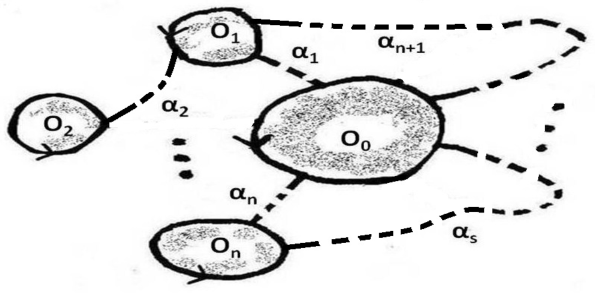

Figure 5: A chord graph

The pair $(o; \alpha)$ is called a *chord graph*, the trivial link o the *based loops*, and the arcs α the *chords*. The ribbon surface-link F given by the pair $(o; \alpha)$ is denoted by $F = F(o; \alpha)$. The notation $\hat{F}^2_{-2}(o, \alpha)$ given in the proof of Lemma 2.2 is also used when we emphasize that the disk systems are in $\mathbf{R}^3[\pm 2]$, the upper bands are in $\mathbf{R}^3[1]$ and the lower bands are in $\mathbf{R}^3[-1]$.

We note that the chord graph $(o; \alpha)$ is nothing but a trivalent spatial graph obtained from a trivial link by adding a finite number of mutually disjoint arcs. A *ribbon chord diagram* or simply a *chord diagram* is a spatial graph diagram $C(o; \alpha)$

of a chord graph $(o;\alpha)$. In an earlier paper [12], the chord graph is called a *disk-arc presentation* of a ribbon-surface-link.

We note that the diagram on the based loops in the chord diagram $C(o;\alpha)$ may have crossings since it is exactly a diagram of a trivial link. See Fig. 6 for a chord diagram whose based loops have crossings.

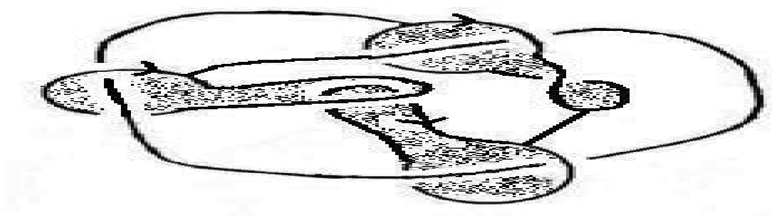

Figure 6: A chord diagram with crossed based loops

In the band presentations of the chords, the bands should be twisted so that the realizing surface is oriented. For example, as band presentations of the chords in Fig. 7, the chord of (1) must be replaced by a $2m$-half-twist band whereas the chord of (2) must be replaced by a $(2m+1)$-half-twist band, for any integer m, to obtain an oriented surface-link. Then we note that the equivalence class of the resulting surface-link is independent of a choice of the twists by [6, Lemma 1.4], which gives a merit adopting a chord rather than a band to represent a ribbon surface-link. Although every based loop in a chord graph is oriented, the arrow is omitted unless we emphasize the orientation.

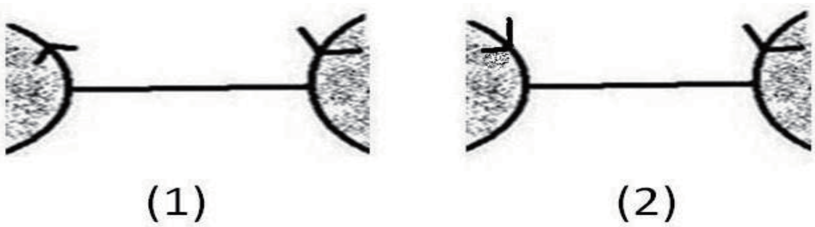

Figure 7: A difference on chords

If an oriented compact 1-manifold ℓ is properly embedded in the upper-half 3-space

$$\mathbf{R}^3_+ = \{(x_1,x_2,x_3) \in \mathbf{R}^3 |\, x_3 \geqq 0\},$$

then the surface-link $F(\ell)$ in $\mathbf{R}^4$ is constructed from ℓ by the mapping

$$(x_1,x_2,x_3) \to (x_1,x_2,x_3\cos\theta, x_3\sin\theta) |\, 0 \leqq \theta \leqq 2\pi\},$$

where every arc or loop component in ℓ changes into an S^2-component or a torus-component in $F(\ell)$, respectively. The surface-link $F(\ell)$ is a ribbon surface-link (see [17]), called the *spun surface-link* of ℓ, and this construction is called *Artin's spinning construction* (see [1]). A chord diagram C_D of the ribbon surface-link $F(\ell)$ is obtained from any diagram D of ℓ in $\mathbf{R}^3_+$ by replacing a neighborhood of every crossing point of D with any one of the two diagrams in the right hand of Fig. 8 and every endpoint of an arc component of ℓ with a based loop (with any orientation) attaching to the endpoint. See Fig. 9 for an illustration of this replacement, where the equality in Fig. 9 will be seen from the moves M_0, M_1 and M_2 on chord diagrams introduced in Section 3.

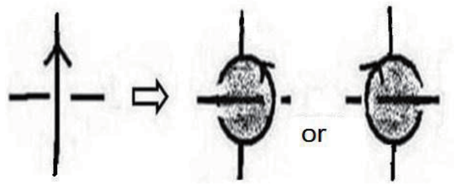

Figure 8: Transforming a neighborhood of a crossing point into a part of a chord diagram

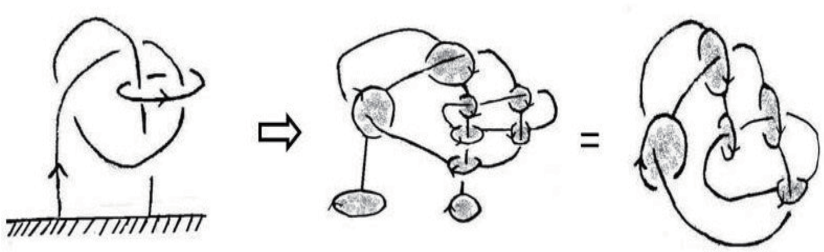

Figure 9: Transforming a diagram of a 1-manifold into a chord diagram

The following example concerns a ribbon torus-knot due to T. Yajima [23].

Example 2.5. Yajima's ribbon torus-knot is described in Fig. 10. As it is explained in [23], the spun trefoil S^2-knot (in the left side of Fig. 10) is obtained by cutting the chord α_1 and the ribbon S^2-knot (in the right side of Fig. 10) constructed from the standard ribbon disk of the Stevedore knot (6_1) is obtained by cutting the chord α_2.

Every virtual link diagram D (see [10]) is transformed into a chord diagram C_D by replacing a neighborhood of every real crossing with any one of the two diagrams

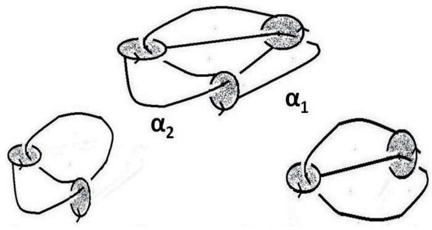

Figure 10: Yajima's ribbon torus-knot

in the right hand of Fig. 8 and then by replacing a neighborhood of every virtual crossing by any one of the two diagrams in the right hand of Fig. 11.

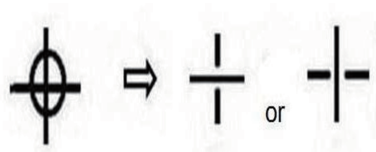

Figure 11: Transforming a neighborhood of a virtual crossing point into a part of a chord diagram

The based loops of the chord diagram C_D bound mutually disjoint disks in the plane and every based loop of C_D is passed through by a chord. In general, such a chord diagram is called a *regular chord diagram*. Further, if every chord of C_D is oriented as it is illustrated in Fig. 12, then every chord of C_D is compatibly oriented. In general, such a regular chord diagram is called an *oriented regular chord diagram*. For an oriented regular chord diagram, an orientation to one chord is sufficient to specify the orientations on all the chords. The chord system of a chord diagram is *simple* if there is no crossing among the chords. If D is a link diagram, then the chord diagram C_D is an oriented regular chord diagram with simple chord system, and if D is a virtual link diagram, then the chord diagram C_D is an oriented regular chord diagram.

To avoid ambiguities on an oriented regular chord diagram C_D constructed from a virtual link diagram D, we also use the replacements given in Fig. 13. Then the diagram resulting from C_D is called the *flat chord diagram* of C_D and denoted by $\bar{C}_D$. It is noted that the flat chord diagram $\bar{C}_D$ recovers the virtual link diagram D uniquely by taking the upper arcs on the based loops of any chord diagram C_D inducing $\bar{C}_D$ and then by replacing the crossing points on the chords of $\bar{C}_D$ with the virtual crossing points.

Let $\mathcal{D}$ be the set of link diagrams, and $\mathcal{D}_{\mathcal{V}}$ be the set of virtual link diagrams. Then we have $\mathcal{D} \subset \mathcal{D}_{\mathcal{V}}$. Let $\bar{\mathcal{C}}_{\mathcal{D}}$ be the set of flat chord diagrams obtained from the

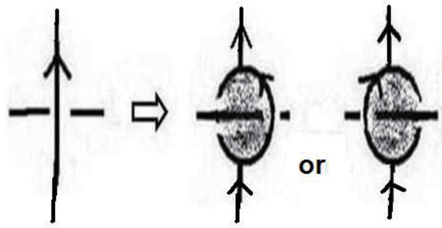

Figure 12: An oriented chord diagram

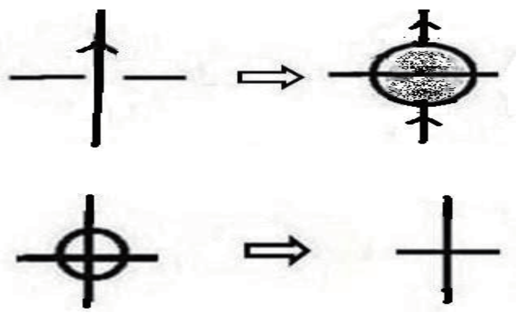

Figure 13: Transforming a neighborhood of a crossing point and a virtual crossing point into a flat chord diagram

set $\mathcal{D}$ of link diagrams, and $\bar{\mathcal{C}}_{\mathcal{V}}$ the set of flat chord diagrams obtained from the set $\mathcal{D}_{\mathcal{V}}$ of virtual link diagrams. We also have $\bar{\mathcal{C}}_{\mathcal{D}} \subset \bar{\mathcal{C}}_{\mathcal{V}}$. Let

$$\iota : (\mathcal{D}_{\mathcal{V}}, \mathcal{D}) \longrightarrow (\bar{\mathcal{C}}_{\mathcal{V}}, \bar{\mathcal{C}}_{\mathcal{D}})$$

be the bijection defined by sending every D to $\bar{C}_D$. The Reidemeister moves of classical, virtual and welded virtual link diagrams are transformed into moves on the flat chord diagrams as they are given in Fig. 14, where the Reidemeister moves $R_1 - R_8$ change into the moves $cR_1 - cR_8$ on the flat chord diagrams, where orientations of the chords, naturally preserved are omitted.

Note that the sets of links, virtual links and welded virtual links are given by the quotient sets $\mathcal{D}/(R_1 - R_3)$, $\mathcal{D}_{\mathcal{V}}/(R_1 - R_7)$ and $\mathcal{D}_{\mathcal{V}}/(R_1 - R_8)$, respectively. The following proposition is direct.

Proposition 2.6. The bijection ι induces bijections:

$$\iota_* : \mathcal{D}/(R_1 - R_3) \longrightarrow \bar{\mathcal{C}}_{\mathcal{D}}/(cR_1 - cR_3),$$
$$\iota_* : \mathcal{D}_{\mathcal{V}}/(R_1 - R_7) \longrightarrow \bar{\mathcal{C}}_{\mathcal{V}}/(cR_1 - cR_7),$$
$$\iota_* : \mathcal{D}_{\mathcal{V}}/(R_1 - R_8) \longrightarrow \bar{\mathcal{C}}_{\mathcal{V}}/(cR_1 - cR_8).$$

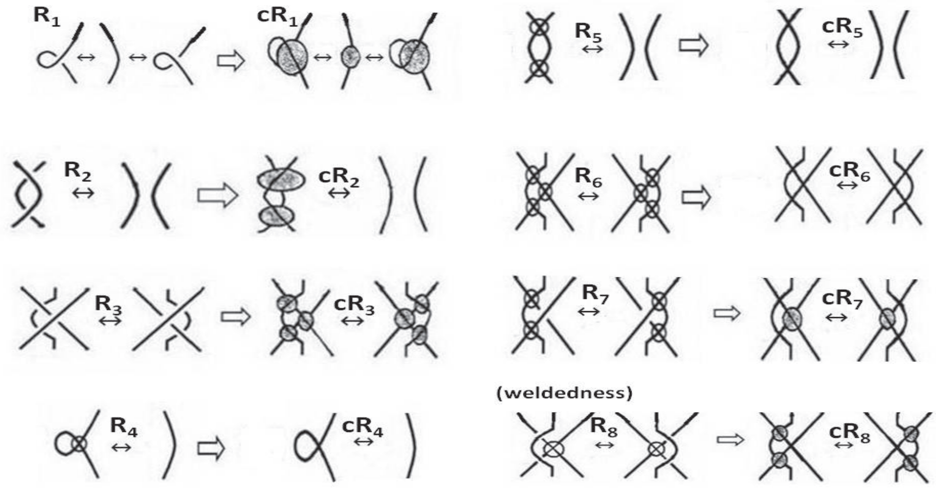

Figure 14: Replacements of the Reidemeister moves

The following proposition is known by [3] for (1) and [20] for (2).

Proposition 2.7. (1) The quotient map

$$\mathcal{D}/(R_1 - R_3) \to \mathcal{D}_{\mathcal{V}}/(R_1 - R_7)$$

is injective.
(2) The composite quotient map

$$\mathcal{D}/(R_1 - R_3) \to \mathcal{D}_{\mathcal{V}}/(R_1 - R_7) \to \mathcal{D}_{\mathcal{V}}/(R_1 - R_8)$$

is injective, whereas the quotient map

$$\mathcal{D}_{\mathcal{V}}/(R_1 - R_7) \to \mathcal{D}_{\mathcal{V}}/(R_1 - R_8)$$

is not injective.

Non-injectivity of the quotient map

$$\mathcal{D}_{\mathcal{V}}/(R_1 - R_7) \to \mathcal{D}_{\mathcal{V}}/(R_1 - R_8)$$

using flat chord diagrams is shown by Fig. 15.

The following corollary is direct from Proposition 2.7.

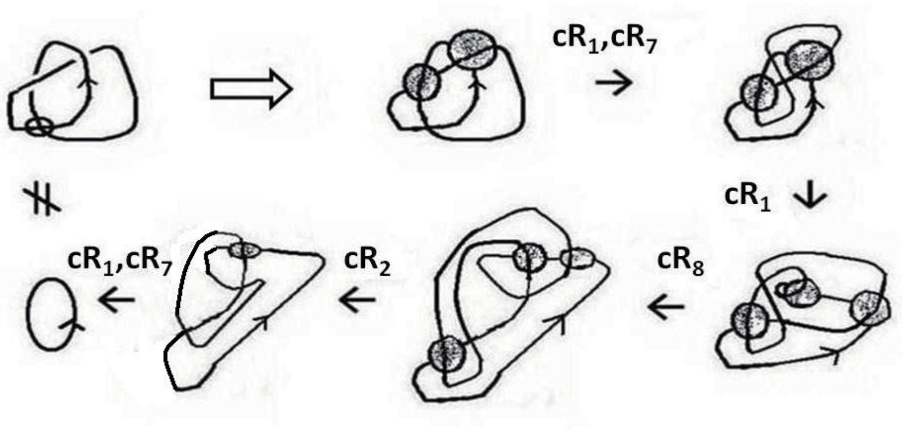

Figure 15: Non-injectivity of the map $\mathcal{D}_{\mathcal{V}}/(R_1 - R_7) \to \mathcal{D}_{\mathcal{V}}/(R_1 - R_8)$

Corollary 2.8. The composite map

$$\bar{\mathcal{C}}_{\mathcal{D}}/(cR_1 - cR_3) \to \bar{\mathcal{C}}_{\mathcal{V}}/(cR_1 - cR_7) \stackrel{non-injective}{\to} \bar{\mathcal{C}}_{\mathcal{V}}/(cR_1 - cR_8)$$

is injective.

3. Moves on chord diagrams

In this section, three kinds of moves M_0, M_1 and M_2 on the set $\mathcal{C}$ of chord diagrams are introduced such that the moves $cR_1 - cR_8$ are consequences of the moves M_0, M_1 and M_2.

Move $\mathbf{M}_0$. This move consists of the Reidemeister moves R_1, R_2, R_3, gR_4, gR_5 as spatial trivalent graphs, illustrated in Fig. 16.

We note that any two arcs in the three arcs together with a vertex or any arc in Fig. 16 can be taken to belong to a based loop although the orientation and the shadow of the based loop are omitted there.

Move $\mathbf{M}_1$. This move is the *fusion-fission move*, illustrated in Fig. 17, where the fusion operation is done only for a chord between different based loops.

The following lemma is obtained.

Lemma 3.1. Under the use of the move M_0, the move M_1 is equivalent to the combination move of the *elementary fusion-fission move* $M_{1.0}$, the *chord slide move*

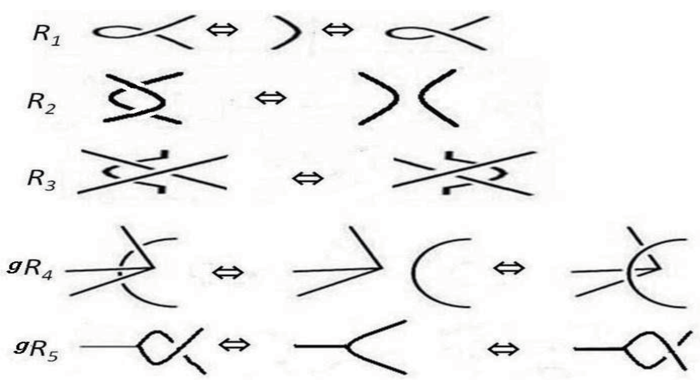

Figure 16: Move M_0: Reidemeister moves R_1, R_2, R_3, gR_4, gR_5 for trivalent graph diagrams

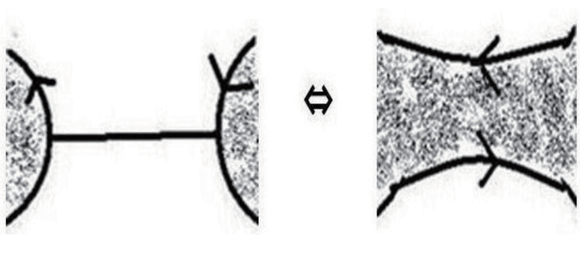

Figure 17: Fusion-fission M_1

$M_{1.1}$ and the *chord pass move* $M_{1.2}$ illustrated in Fig. 18. The *birth-death move* illustrated in Fig. 19 is obtained from these moves, unless a closed chord is involved.

As a convention, a closed chord is regarded as a chord with a based loop constructed from the birth-death move.

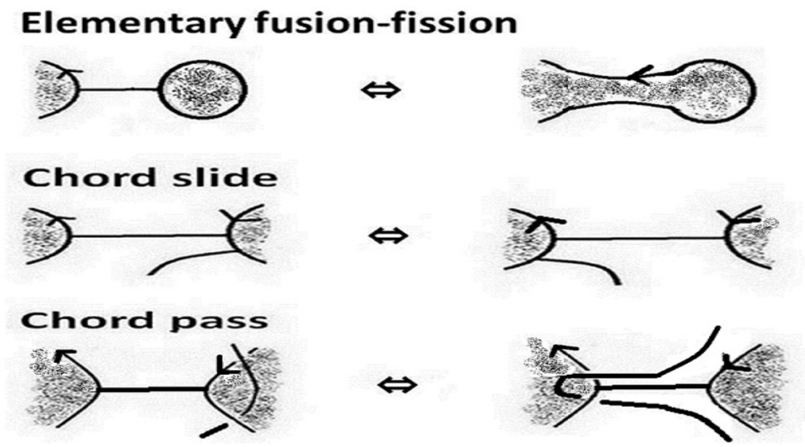

Figure 18: Elementary fusion-fission $M_{1.0}$, Chord slide $M_{1.1}$ and Chord pass $M_{1.2}$

Proof of Lemma 3.1. The move M_1 implies the moves $M_{1.0}$, $M_{1.1}$ and $M_{1.2}$. To obtain the converse, we assume by using M_0 that the disks bounded by the based loops in the left figure of Fig. 17 are embedded in the plane and disjoint from the other based loops. By using $M_{1.1}$ and $M_{1.2}$, a situation to apply $M_{1.0}$ is created, so that the right figure of Fig. 17 is obtained. Next, we assume by using M_0 that the disk bounded by the based loop in the right figure of Fig. 17 is embedded in the plane and disjoint from the other based loops. By $M_{1.0}$, a situation to apply $M_{1.1}$ and $M_{1.2}$ is created, so that the left figure of Fig. 17 is obtained. Thus, the desired equivalence is shown. Next, to obtain the birth-death move from M_1, we take the chord of the left figure of Fig. 19 near the attaching point of the chord to a based loop to obtain the right figure of Fig. 19 by using M_1. The resulting based loop can slide along the chord by using M_0. Thus, we obtain the birth-death move. □

Move $\mathbf{M}_2$. This move consists of moves on chords, illustrated in Fig. 20.

The following observation is easily obtained.

Observation 3.2. The moves $cR_1 - cR_8$ on the set $\mathcal{C}_{\mathcal{V}}$ of oriented chord diagrams are the consequences of the moves M_0, M_1, M_2.

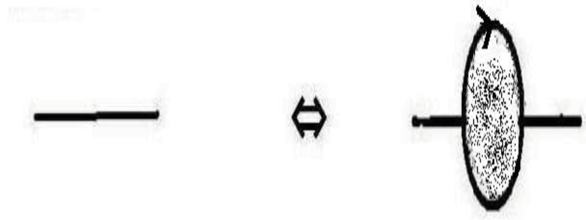

Figure 19: The birth-death move

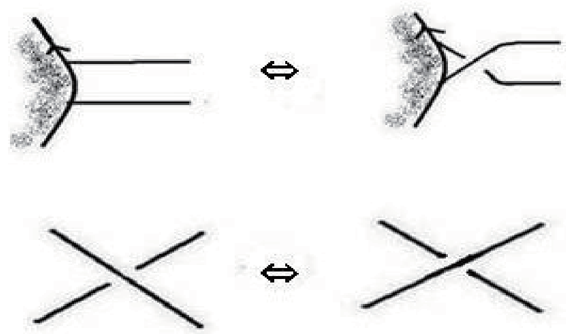

Figure 20: Chord moves M_2

The following proposition is given by S. Satoh [21].

Proposition 3.3. Let $\mathcal{C}_1$ be the subset of $\mathcal{C}$ represented by ribbon torus-links. Then the operation recovering any chord diagram C_D from the flat chord diagram $\bar{C}_D$ for every virtual link diagram D induces a surjection

$$\tau : \bar{\mathcal{C}}_{\mathcal{V}}/(cR_1 - cR_8) \to \mathcal{C}_1/(M_0, M_1, M_2).$$

Thus, there is a surjection from the set of welded virtual links onto the set of ribbon torus-links. Further, every arrow of the following sequence

$$\mathcal{D}/(R_1 - R_3) \to \mathcal{D}_{\mathcal{V}}/(R_1 - R_7) \to \mathcal{D}_{\mathcal{V}}/(R_1 - R_8) \overset{\iota_*}{\cong} \bar{\mathcal{C}}_{\mathcal{V}}/(cR_1 - cR_8) \overset{\tau}{\to} \mathcal{C}_1/(M_0, M_1, M_2)$$

preserves the fundamental group presentations.

Proof of Proposition 3.3 from our viewpoint. Observation 3.2, it suffices to show that τ is a surjection. By the move M_0, a chord diagram $C \in \mathcal{C}_1$ is deformed into a chord diagram C' so that the based loops bound mutually disjoint disks in the plane and the crossings among the chords arise outside the disks. Since C' represents a ribbon torus-link, by the chord slide $M_{1.1}$, the chord diagram C' is deformed into a chord diagram C'' so that every based loop of C'' has just two end points. A based loop where no chord passes through can be removed by the birth-death move. Thus, by the fusion-fission move M_1, C'' is deformed into a regular chord diagram. If the regular chord diagram C'' is oriented, then we have $C'' = C_D$ for a virtual link diagram D. The flat chord diagram $\bar{C}_D$ is sent to C in $\mathcal{C}_1/(M_0, M_1, M_2)$. If the chord diagram C'' is non-orientable, then C'' can be changed into an oriented regular chord diagram by the move M_0 as it is shown in Fig. 21. The reason why the fundamental group presentations are preserved comes from the fact that the group relations of a virtual link diagram are exactly equal to the group relations of a ribbon torus-link diagram (cf. [23]), as they are shown in Fig. 22. This completes the proof of Proposition 3.3. □

The following observation is more or less known.

Observation 3.4. The map $\tau : \bar{\mathcal{C}}_{\mathcal{V}}/(cR_1 - cR_8) \to \mathcal{C}_1/(M_0, M_1, M_2)$ is not injective.

Proof of Observation 3.4. By construction of a ribbon surface-link, every chord diagram $C(o; \alpha)$ and the inversed mirror image $C(-o; \alpha)^*$ represent the equivalent ribbon surface-links. On the other hand, there are many links L in $\mathbf{R}^3$, which is not equivalent to the inversed mirror image (=the negative amphicheiral link) $-L^*$ of L (for example, take the trefoil knot as L) which are still distinct as welded virtual links by [20], completing the proof of Observation 3.4. □

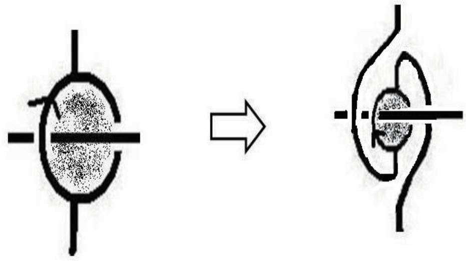

Figure 21: Changing a non-orientable chord into an oriented chord

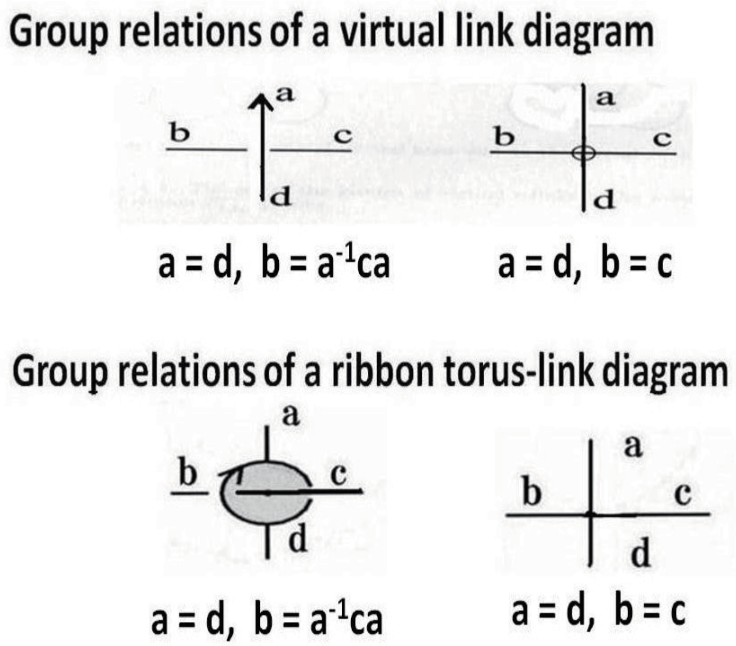

Figure 22: Group relations

4. Faithful equivalence on ribbon surface-link and the main result

To state the definition of a faithful equivalence, let $h(\alpha)$ be the 1-handles along the chords α, used for the construction of a ribbon surface-link $F(o;\alpha)$. Let $F(o;h(\alpha)) = F(o;\alpha) \cup h(\alpha)$. A ribbon surface-link $F(o;\alpha)$ is *faithfully equivalent* to a ribbon surface-link $F(o';\alpha')$ if there is an equivalence $f : \mathbf{R}^4 \to \mathbf{R}^4$ sending $F(o;\alpha)$ to $F(o';\alpha')$ and every meridian (i.e., belt 1-sphere) of the 1-handles $h(\alpha)$ to a null-homotopic curve in $F(o';h(\alpha'))$.

To see that the faithful equivalence is an equivalence relation, first assume that $F(o;\alpha)$ be a ribbon surface-knot. Let $\pi_1(F(o;\alpha))_\wedge$ be the quotient of the fundamental group $\pi_1(F(o;\alpha))$ by the normal subgroup generated normally by meridians of the 1-handles $h(\alpha)$. The group $\pi_1(F(o;\alpha))_\wedge$ is isomorphic to the group $\pi_1(F(o;h(\alpha)))$ which is a free group of rank equal to the genus of the surface $F(o;\alpha)$. By definition, the faithful equivalence $f : \mathbf{R}^4 \to \mathbf{R}^4$ induces an epimorphism $f_\# : \pi_1(F(o;\alpha))_\wedge \to \pi_1(F(o';\alpha'))_\wedge$, which is an isomorphism since they are free groups of the same rank. Thus, the inverse equivalence f^{-1} gives a faithful equivalence from $F(o';\alpha')$ to $F(o;\alpha)$ and hence the faithful equivalence on ribbon surface-knots is an equivalence relation. Considering this argument componentwise, we see that the faithful equivalence on ribbon surface-links is an equivalence relation. We also note that the ribbon surface-link $F(o;\alpha)$ is uniquely constructed from a chord graph $(o;\alpha)$ up to faithful equivalences.

The main theorem of this paper is stated as follows:

Theorem 4.1. Two ribbon surface-links $F(o;\alpha)$ and $F(o';\alpha')$ are faithfully equivalent if and only if the chord diagram $C(o';\alpha')$ is obtained from the chord diagram $C(o;\alpha)$ by a finite number of the moves M_0, M_1, M_2.

Since any faithful equivalence on ribbon S^2-links is equivalent to an equivalence, this result answers a question of Y. Nakanishi's paper [19] and Y. Marumoto's paper [17] (cf. [11, p.186]) asking on ribbon S^2-knots affirmatively. We also mention that a similar result is claimed by B. Winter [22] in a different way (unpublished).

The moves M_0, M_1, M_2 do not alter the faithful equivalence class of a ribbon surface-link. Thus, the if part is trivial. *Throughout the remainder of this section, the proof of the only if part of Theorem 4.1 will be done.* First, assume that the ribbon surface-links $F(o;\alpha) = \hat{F}^2_{-2}(o;\alpha)$ and $F(o';\alpha') = \hat{F}^2_{-2}(o';\alpha')$ are ribbon surface-knots. Let $F^2_{-2}(o;\alpha)$ and $F^2_{-2}(o';\alpha')$ be the surfaces obtained from $\hat{F}^2_{-2}(o;\alpha)$ and $\hat{F}^2_{-2}(o';\alpha')$ by removing the upper and lower disk systems, respectively. By the moves M_1 and M_2, we can assume the following (1)-(3).

(1) The based loops o and o' are identical: $o = o'$ and have the $n+1$ components o_i $(i = 0,1,2,\dots,n)$.
(2) The chords α and α' have the same number of chords α_j and α'_j with identical

boundaries $\partial\alpha_j = \partial\alpha'_j$ for all j ($j = 1, 2, \ldots, s$),
(3) The chords α connect the based loops o as in Fig. 23. Namely, for every j with $1 \leqq j \leqq n$ the chord α_j joins the based loop o_j to the based loop o_0, referred to as a *non-self-connecting chord*, and for every j with $n+1 \leqq j \leqq s$ the chord α_j joins the based loop o_0 itself, referred to as a *self-connecting chord*.

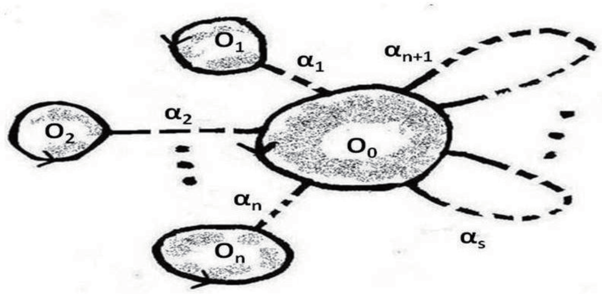

Figure 23: A specification of the chords α joining the based loops o

We use the following lemma, well-known by the uniqueness of regular neighborhoods and the isotopy extention theorem in the piecewise-linear topology (cf. Hudson [7]).

Lemma 4.2. Let (D^4, D^2) be the standard (4,2)-disk pair. For any two disjoint disks d_i ($i = 0, 1, \ldots, n$) and d'_i ($i = 0, 1, \ldots, n$) in the disk interior $\mathrm{int}(D^2)$ whose complement $\mathrm{cl}(D^2 \setminus (\cup_{i=1}^{n} d_i \cup d'_i))$ is a 2-manifold, there is a self-homeomorphism $g : (D^4, D^2) \to (D^4, D^2)$ such that $g|\, \partial D^4 = 1$ and $g(d_i) = d'_i$ for every i ($i = 0, 1, \ldots, n$). Further, if there is an identification of the disks d_i and d'_i with the orientations induced from an orientation of D^2, then we can take $g|\, d_i = 1$.

In fact, by the assumption of Lemma 4.2, the disks d_i ($i = 0, 1, \ldots, n$) and d'_i ($i = 0, 1, \ldots, n$) are considered as piecewise-linearly embedded disks in D^2 where we can apply the uniqueness of regular neighborhoods and the isotopy extention theorem. By Lemma 4.2, we have the following lemma.

Lemma 4.3. There is a faithful equivalence

$$f : \mathbf{R}^4 \to \mathbf{R}^4$$

from $\hat{F}^2_{-2}(o;\alpha))$ to $\hat{F}^2_{-2}(o;\alpha')$ with $f|\, \mathbf{R}^3(-\infty, -3] \cup \mathbf{R}^3[3, +\infty) = 1$ such that

$$f|\, d[-2] \cup u[-2, 1] \cup o[1, 2] \cup d[2] = 1$$

for the union u of an arc $u_i \subset o_i \setminus o_i \cap \alpha$ for every i.

Proof of Lemma 4.3. Since a surface-link is compact, the faithful equivalence is given by an orientation-preserving homeomorphism $h : \mathbf{R}^4 \to \mathbf{R}^4$ with compact support. Thus, we can assume that $h|\,\mathbf{R}^3(-\infty,-3] \cup \mathbf{R}^3[3,+\infty) = 1$. Choose a 2-disk D^2_1 in $\hat{F}^2_{-2}(o;\alpha')$ containing the disk system $f(d[-2]\cup u[-2,1]\cup o[1,2]\cup d[2])$ and a disjoint small 2-disk Δ_1. Since $\hat{F}^2_{-2}(o;\alpha')$ is smoothly embedded in $\mathbf{R}^3[-3,3]$, the disk D^2_1 is regarded as a standard 2-disk in a 4-disk D^4_1 in $\mathbf{R}^3[-3,3]$ with $D^4_1\cap \hat{F}^2_{-2}(o;\alpha') = D^2_1$. By Lemma 4.2, the disk system $f(d[-2]\cup u[-2,1]\cup o[1,2]\cup d[2])$ is deformed into a previously specified disk system in Δ_1 by a homeomorphism $g_1 : D^4_1 \to D^4_1$ with $g_1(D^2_1) = D^2_1$ and $g_1|\,\partial D^4_1 = 1$. Let D^2_2 be a 2-disk in $\hat{F}^2_{-2}(o;\alpha')$ containing the disk system $d[-2] \cup u[-2,1] \cup o[1,2] \cup d[2]$ and a disjoint 2-disk Δ_2, and D^4_2 a 4-disk in $\mathbf{R}^3[-3,3]$ with D^2_2 a standard 2-disk and $D^4_2 \cap \hat{F}^2_{-2}(o;\alpha') = D^2_2$. By Lemma 4.2, the disk system $d[-2]\cup u[-2,1]\cup o[1,2]\cup d[2]$ is deformed into a previously specified disk system in Δ_2 by a homeomorphism $g_2 : D^4_2 \to D^4_2$ with $g_2(D^2_2) = D^2_2$ and $g_2|\,\partial D^4_2 = 1$. Let $\Delta_1 \cap \Delta_2 = \emptyset$. Choose a 2-disk D^2_3 in $\hat{F}^2_{-2}(o;\alpha')$ containing $\Delta_1 \cup \Delta_2$. Let D^4_3 be a 4-disk in $\mathbf{R}^3[-3,3]$ with D^2_3 as a standard 2-disk and $D^4_3 \cap \hat{F}^2_{-2}(o;\alpha') = D^2_3$. By Lemma 4.2, a previously specified disk system in Δ_1 is also deformed into a previously specified disk system in Δ_2 by a homeomorphism $g_3 : D^4_3 \to D^4_3$ with $g_3(D^2_3) = D^2_3$ and $g_3|\,\partial D^4_3 = 1$. Let $g^+_i : \mathbf{R}^4 \to \mathbf{R}^4$ be the homeomorphism obtained from g_i by the identity extension for $i = 1,2,3$. Then the composition $f = (g^+_2)^{-1} g^+_3 g^+_1 h$ is a desired faithful homeomorphism because g_i $(i = 1,2,3)$ give isotopic deformations on $\hat{F}^2_{-2}(o;\alpha')$. $\square$

We put copies of the chords α and α' in the upper bands of $\hat{F}^2_{-2}(o;\alpha)$ and $\hat{F}^2_{-2}(o;\alpha')$ in $\mathbf{R}^3[1]$ which are denoted by $\bar{\alpha}$ and $\bar{\alpha}'$, respectively. Let $\Gamma(\alpha)$ be the graph obtained from the chord graph $(o;\alpha)$ in $\mathbf{R}^3$ by deleting the interior of u, and $\Gamma(\alpha')$ the graph obtained similarly from the chord graph $(o;\alpha')$ in $\mathbf{R}^3$ (see Fig. 24). Let $\bar{\Gamma}(\alpha)$ and $\bar{\Gamma}(\alpha')$ be the graphs obtained by putting $\Gamma(\alpha)$ and $\Gamma(\alpha')$ in $F^2_{-2}(o;\alpha) \cap \mathbf{R}^3[1]$ and $F^2_{-2}(o;\alpha') \cap \mathbf{R}^3[1]$, respectively. Then we have the following lemma:

Lemma 4.4. The faithful equivalence $f : \mathbf{R}^4 \to \mathbf{R}^4$ in Lemma 4.3 induces a map

$$f_* : \bar{\Gamma}(\alpha) \to \bar{\Gamma}(\alpha')$$

preserving the degree one vertices graph-componentwise and inducing an isomorphism on the fundamental groups of the corresponding components.

Proof of Lemma 4.4. First, assume that G and G' are ribbon surface-knots. Let $G = \hat{F}^2_{-2}(o;\alpha)$ and $G' = \hat{F}^2_{-2}(o;\alpha')$. Also, let $G_h = G \cup h(\alpha)$ and $G'_h = G' \cup h(\alpha')$. Let

$$\Delta = d[-2] \cup u[-2,2] \cup d[2], \quad E = \mathrm{cl}(G \setminus \Delta) \quad \text{and} \quad E' = \mathrm{cl}(G' \setminus \Delta).$$

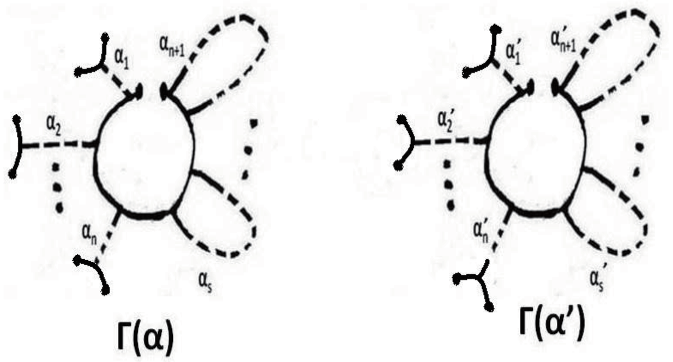

Figure 24: The graph Γ

Also, let

$$E_h = E \cup h(\alpha) \quad \text{and} \quad E'_h = E' \cup h(\alpha').$$

We note that

$$\bar{\Gamma}(\alpha) \subset E \subset E_h, \quad \bar{\Gamma}(\alpha') \subset E' \subset E'_h$$

and there are strong deformation retractions $E_h \to \bar{\Gamma}(\alpha)$ and $E'_h \to \bar{\Gamma}(\alpha')$. Since f defines a homeomorphism $E \to E'$, we see from the inclusion map $\bar{\Gamma}(\alpha) \subset E$ and the retraction $E'_h \to \bar{\Gamma}(\alpha')$ that f defines a map $f_* : \bar{\Gamma}(\alpha) \to \bar{\Gamma}(\alpha')$ uniquely up to homotopy which keeps the degree one vertices. Also, note that the fundamental groups $\pi_1(\bar{\Gamma}(\alpha))$ and $\pi_1(\bar{\Gamma}(\alpha'))$ are free groups of rank $s-n$ with bases represented by the self-connecting chords $\bar{\alpha}_j$ and $\bar{\alpha}'_j$ ($j = n+1, n+2, \ldots, s$), respectively. To see that f_* induces an isomorphism on the fundamental groups, let $m \subset E$ be a meridian of the 1-handles $h(\alpha)$. By the faithfulness of f, the image $f(m) \subset E'$ is null-homotopic in G'_h. For the disk system d bounded by o in $\mathbf{R}^3$ which is used for the construction of G', let $c : o \times [0, \varepsilon] \to d$ be a boundary collar of o in d with $c(x, 0) = x$ ($\forall x \in o$) for a sufficiently small positive number ε. For the 2-sphere $S^2 = d[-2] \cup o[-2, 2] \cup d[2]$, let

$$S^2_c = d[-2, -2+\varepsilon] \cup c(o \times [0, \varepsilon])[-2, 2] \cup d[2, 2-\varepsilon]$$

be a 3-manifold naturally homeomorphic to $S^2 \times [0, \varepsilon]$. We assume that the 1-handles $h(\alpha')$ meet the compact 3-manifold S^2_c only in the attaching disks to $o[-2, 2]$.

The loop $f(m)$ bounds a generic piecewise-linear singular disk D_* in the compact 3-manifold $G'_{h,c} = G'_h \cup S^2_c$. Let

$$\Delta_c = d[-2, -2+\varepsilon] \cup c(u \times [0, \varepsilon])[-2, 2] \cup d[2, 2-\varepsilon]$$

be a 3-manifold naturally homeomorphic to $\Delta \times [0, \varepsilon]$. Let $J = c(p \times [0, \varepsilon])$ be the arc for an interior point p of u which is proper in S^2_c. Since Δ_c is a regular neighborhood of J in S^2_c and J can be assumed to meet the singular disk D_* in a part apart from the singularity transversely, we can assume from the uniqueness of regular neighborhoods that the disk D_* meets Δ_c in disks $P(\Delta)$ parallel to the disk Δ in Δ_c. Note that the disks $P(\Delta)$ are contained in 2-spheres $P(S^2)$ parallel to the 2-sphere S^2 in S^2_c. Replacing the disks $P(\Delta)$ with the complementary disks $\mathrm{cl}(P(S^2) \setminus P(\Delta))$, we see that the loop $f(m)$ bounds a singular disk D'_* in the 3-manifold $\mathrm{cl}(G'_{c,h} \setminus \Delta_c)$ of which E'_h is a strong deformation retract. Thus, the loop $f(m)$ is null-homotopic in E'_h. This implies that the map $f_* : \bar{\Gamma}(\alpha) \to \bar{\Gamma}(\alpha')$ induces an epimorphism on the free fundamental groups of the same rank, meaning an isomorphism. When G and G' are ribbon surface-links, the same conclusion is obtained by considering the argument above componentwise. □

On the non-self-connecting chords, it is seen from Lemma 4.4 that after the endpoints of every non-self-connecting chord α'_j are moved along the arcs $\mathrm{cl}(o \setminus u)$ and the other chords $\alpha'_{j'}$ $(j' \neq j)$, the image $f(\bar{\alpha}_j)$ of every non-self-connecting chord $\bar{\alpha}_j$ is homotopically deformed into the chord $\bar{\alpha}'_j$ by a homotopy in $\bar{\Gamma}(\alpha')$ relative to the endpoints of $\bar{\alpha}'_j$.

On the self-connecting chords, we use the fact in [18] that every automorphism of a free group of a finite rank is generated by the *elementary Nielsen transformations*, meaning

(1) Exchange of two basis elements,
(2) Replacement of a basis element by its inverse, and
(3) Replacement of a basis element by the product of it and another basis element.

By this fact and Lemma 4.4, after finitely many processes of sliding the endpoints of every self-connecting chord α'_j along the arcs $\mathrm{cl}(o \setminus u)$ and some of the other chords $\alpha'_{j'}$ $(j' \neq j)$, the image $f(\bar{\alpha}_j)$ of every self-connecting chord $\bar{\alpha}_j$ is homotopically deformed into the chord $\bar{\alpha}'_j$ by a homotopy in $\bar{\Gamma}(\alpha')$ relative to the endpoints of $\bar{\alpha}'_j$. Thus, we have the following lemma.

Lemma 4.5. After a finite number of the moves M_0, M_1, M_2 on the chord diagrams $C(o;\alpha)$ and $C(o;\alpha')$, the image $f(\bar{\alpha})$ is homotopic to $\bar{\alpha}'$ in $\mathbf{R}^3[-3,3]$ by a homotopy relative to the cylinders $o[-3,3]$.

The following lemma is needed to compare the chords α with the chords α'.

Lemma 4.6. The homeomorphism $f : \mathbf{R}^3[-3,3] \to \mathbf{R}^3[-3,3]$ is isotopic to a homeomorphism $f' : \mathbf{R}^3[-3,3] \to \mathbf{R}^3[-3,3]$ extending the homeomorphism

$$f|\, F^2_{-2}(o;\alpha) : F^2_{-2}(o;\alpha) \to F^2_{-2}(o;\alpha')$$

such that

$$f'|\, o[-3] \cup u[-3,3] \cup o[3] = 1.$$

Proof of Lemma 4.6. Let p be the set of an interior point of the arc u_i for every i. By the result of Freedman-Quinn [2, 8.1A], we may consider that the arcs $f(p[2,3])$ are smooth arcs although the homeomorphism f is not a diffeomorphism or a piecewise-linear homeomorphism. The intersection $f(p[2,3]) \cap \mathbf{R}^3[-3,2]$ is a disjoint union of the points $f(p[2]) = p[2]$ and compact arcs I with the boundaries ∂I in $\mathbf{R}^3[2]$. Since the natural homomorphism

$$\pi_1(\mathbf{R}^3[2] \setminus o[2]) \to \pi_1(\mathbf{R}^3[-3,2] \setminus (F^2_{-2}(o;\alpha') \cup d[-2]))$$

is onto, it can be seen that the arcs I are homotopically deformed into $\mathbf{R}^3[2] \setminus o[2]$ by a homotopy relative to ∂I in $\mathbf{R}^3[-3,2] \setminus (F^2_{-2}(o;\alpha') \cup d[-2])$. By applying the same argument to $f(p[-3,-2])$, we may consider that there is a homeomorphism $f' : \mathbf{R}^3[-3,3] \to \mathbf{R}^3[-3,3]$ which is isotopic to f and extends the homeomorphism $f|\, F^2_{-2}(o;\alpha) : F^2_{-2}(o;\alpha) \to F^2_{-2}(o;\alpha')$ such that

$$f'(p[2,3]) = p[2,3] \quad \text{and} \quad f'(p[-3,-2]) = p[-3,-2].$$

By the uniqueness of regular neighborhoods and an argument of [6, Lemma 1.4], we may have

$$f'(N(p[2,3])) = N(p[2,3]) \quad \text{and} \quad f'(N(p[-3;-2])) = N(p[-3,-2])$$

for normal disk-bundles $N(p[2,3])$ and $N(p[-3,-2])$ of the arcs $p[2,3]$ and $p[-3,-2]$ in $\mathbf{R}^3[2,3]$ and $\mathbf{R}^3[-3,-2]$, respectively. Further, by the uniqueness of regular neighborhoods, the bands $f'(u[-3,-2])$ and $f'(u[2,3])$ are respectively considered to be obtained from the bands $u[-3,-2]$ and $u[2,3]$ by twisting along the arcs $p[-3,-2]$ and $p[2,3]$ in the normal disk-bundles $N(p[-3,-2])$ and $N(p[2,3])$. By a further isotopic deformation of f' keeping $f|\, F^2_{-2}(o;\alpha)$ fixed but granting an isotopic deformation of $f'|\, \mathbf{R}^3[-3] \cup \mathbf{R}^3[3]$, we may have

$$f'|\, o[-3] \cup u[-3,3] \cup o[3] = 1. \quad \square$$

The following corollary is obtained from Lemma 4.6.

Corollary 4.7. After a finite number of the moves M_0, M_1, M_2 on the chord diagrams $C(o;\alpha)$ and $C(o;\alpha')$, the chords α are homotopic to the chords α' in $\mathbf{R}^3$ by a homotopy relative to the based loops o.

Proof of Corollary 4.7. Move the endpoints $\partial\alpha = \partial\alpha'$ of the chords α and α' into the arcs u. For the homeomorphism f' in Lemma 4.6, let $D' \subset \mathbf{R}^3[-3,3]$ be *smoothly immersed* disks which are homotopic to the disks $f'(\alpha[1,3]) \subset \mathbf{R}^3[-3,3]$ by a homotopy in $\mathbf{R}^3[-3,3]$ relative to the boundaries $\partial D' = \partial f'(\alpha[1,3])$. Apart from the arcs $(\partial\alpha)[1,3]$, the disks D' meet the 3-disks $d[-3,3]$ transversely as a compact 1-manifold (avoiding the double points of D') and the disks $\mathrm{cl}(o\setminus u)[-3,3]\subset o[-3,3]$ transversely as the boundaries of proper arcs in the 1-manifold of $D'\cap d[-3,3]$. By using a bi-collar of $d[-3,3]$ in $\mathbf{R}^3[-3,3]$, these proper arcs can be moved out of the 3-disks $d[-3,3]$ outside homotopically to obtain from D' singular disks D'' with $\partial D''=\partial D'$ and $D''\cap o[-3,3]=(\partial\alpha)[1,3]$. Let $(o;\alpha^{f'})$ be the chord graph in $\mathbf{R}^3$ given by $f'((o;\alpha)[3])=(o;\alpha^{f'})[3]$ in $\mathbf{R}^3[3]$. Since $(o;\alpha^{f'})$ is equivalent to the chord graph $(o;\alpha)$ as trivalent spatial graphs, the chord diagram $C(o;\alpha)$ is transformed into any chord diagram $C(o;\alpha^{f'})$ by the move M_0 (see [8, 9, 14] for this proof). By a homotopy from $f'(\bar\alpha)=f(\bar\alpha)$ to $\bar\alpha'$ in $\mathbf{R}^3[-3,3]$ relative to the cylinders $o[-3,3]$ given by Lemma 4.5, we have singular disks D''' in $\mathbf{R}^3[-3,3]$ bounded by $f(\bar\alpha)\cup\bar\alpha'$. The union $\tilde D=D''\cup D'''\cup\alpha'[-3,1]$ is singular disks in $\mathbf{R}^3[-3,3]$ meeting $o[-3,3]$ only in the arcs $(\partial\alpha)[-3,3]$. The projection of the union $o[-3,3]\cup\tilde D$ into $\mathbf{R}^3$ gives a homotopy from the chords $\alpha^{f'}$ to the chords α' in $\mathbf{R}^3$ relative to the based loops o. □

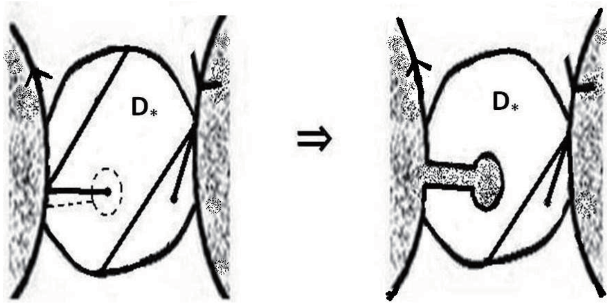

Figure 25: How to eliminate a simple branch type singularity

This corollary and the following lemma complete the proof of Theorem 4.1.

Lemma 4.8. If the chords α are homotopic to the chords α' in $\mathbf{R}^3$ by a homotopy relative to the based loops o, then the chord diagram $C(o;\alpha')$ is obtained from the chord diagram $C(o;\alpha)$ by a finite number of the moves M_0, M_1 and M_2.

Proof of Lemma 4.8. By the move M_0, the loops $\alpha'\cup-\alpha$ bound piecewise-linear immersed disks D_* whose singularities consist of simple clasp type singularities with end points in the interiors of the chords α and α' and of simple branch type singularities with branch points on the based loops o. The simple clasp type singularities are eliminated by M_0 and M_2. To eliminate the simple branch type singularities, split off the endpoints $\partial\alpha$ of the chords α from the endpoints $\partial\alpha'$ of the chords α' by sliding slightly the endpoints $\partial\alpha$ of the chords α along o to obtain piecewise-linear immersed disks D_{**} avoiding the overlaps of the branch points in D_*. Then every simple branch type singularity is eliminated as it is shown in Fig. 25. In fact, the dotted loop in the left figure of Fig. 25 is a loop surrounding a chord in α or α'. Since the dotted chord in the left figure of Fig. 25 with this loop as a based loop is created by using the chord slide move $M_{1.1}$, the birth-death move (in M_1) and the chord move M_2, the right figure of Fig. 25 is obtained by the fusion-fission move (in M_1). By continuing this process, every simple branch type singularity is eliminated. This completes the proof of Theorem 4.1. □

5. Smooth unknotting of a ribbon surface-knot

Two surface-links F and F' in $\mathbf{R}^4$ are *TOP-equivalent* if there is an orientation-preserving homeomorphism $f : \mathbf{R}^4 \to \mathbf{R}^4$ sending F to F' orientation-preservingly. Two ribbon surface-links $F(o;\alpha)$ and $F(o';\alpha')$ are *faithfully TOP-equivalent* if there is an TOP-equivalence $f : \mathbf{R}^4 \to \mathbf{R}^4$ sending $F^2_{-2}(o;\alpha)$ to $F^2_{-2}(o';\alpha')$ and every meridian of the 1-handles $h(\alpha)$ to a null-homotopic curve in $F^2_{-2}(o';h(\alpha'))$. The faithful TOP-equivalence is also an equivalence relation.

By examining our argument of Section 4, the following theorem can be seen.

Corollary 5.1. If two ribbon surface-links $F(o;\alpha)$ and $F(o';\alpha')$ are faithfully TOP-equivalent, then the chord diagram $C(o';\alpha')$ is obtained from the chord diagram $C(o;\alpha)$ by a finite number of the moves M_0, M_1, M_2.

The following corollary is direct from Corollary 5.1.

Corollary 5.2. Two ribbon surface-links are faithfully TOP-equivalent if and only if they are faithfully equivalent.

A surface-knot F in $\mathbf{R}^4$ is *DIFF-trivial* or *TOP-trivial* respectively, if F bounds a handlebody embedded in $\mathbf{R}^4$ by a smooth embedding or a locally-flat topological embedding. It is proved in [4] and [13] that a surface-knot F in $\mathbf{R}^4$ is TOP-trivial if the fundamental group $\pi_1(\mathbf{R}^4 \setminus F)$ is an infinite cyclic group. By an argument of [4], a TOP-trivial ribbon surface-knot is faithfully TOP-equivalent to a trivial ribbon surface-knot $F(o,\alpha)$ with a chord diagram $C(o,\alpha)$ without crossings. More generally, every TOP-equivalence from a ribbon surface-knot to a trivial ribbon surface-knot is made a faithful TOP-equivalence by composing a self-equivalence $\mathbf{R}^4 \to \mathbf{R}^4$ of the trivial ribbon surface-knot preserving the spin structure of the surface-knot (see S. Hirose [5]). Then, we have the following corollary.

Corollary 5.3. A ribbon surface-knot F is DIFF-trivial if the fundamental group $\pi_1(\mathbf{R}^4 \setminus F)$ is an infinite cyclic group.

This proof corrects an erroneous proof of T. Yanagawa's paper [27] (cf. T. Yajima [25]).

Acknowledgements. This work was supported by JSPS KAKENHI Grant Numbers 24244005, 26287013.

References

[1] E. Artin, Zur Isotopie zweidimensionalen Flächen im R_4, Abh. Math. Sem. Univ. Hamburg 4 (1926), 174-177.

[2] M. H. Freedman and F. Quinn, Topology of 4-manifolds, Princeton Univ. Press (1990).

[3] M. Goussarov, M. Polyak and O. Viro, Finite-type invariants of classical and virtual knots, Topology 39 (2000), 1045-1068.

[4] J. A. Hillman and A. Kawauchi, Unknotting orientable surfaces in the 4-sphere, J. Knot Theory Ramifications 4 (1995), 213-224.

[5] S. Hirose, On diffeomorphisms over surfaces trivially embedded in the 4-sphere, Algebraic and Geometric Topology 2 (2002), 791-824.

[6] F. Hosokawa and A. Kawauchi, Proposals for unknotted surfaces in four-space, Osaka J. Math. 16 (1979), 233-248.

[7] J. F. P. Hudson, Piecewise-linear topology, Benjamin (1969).

[8] S. Kamada, A. Kawauchi and T. Matumoto, Combinatorial moves on ambient isotopic submanifolds in a manifold, J. Math. Soc. Japan 53 (2001),321-331.

[9] L. H. Kauffman, Invariants of graphs in three space, Trans. Amer. Math. Soc. 311 (1989), 697-710.

[10] L. H. Kauffman, Virtual knot theory, European J. Combin. 20 (1999), 663-690.

[11] A. Kawauchi, A survey of knot theory, Birkhäuser (1996).

[12] A. Kawauchi, The first Alexander Z[Z]-modules of surface-links and of virtual links, Heiner Zieschang Gedenkschrift, Geometry and Topology Monographs 14 (2008), 353-371.

[13] A. Kawauchi, Splitting a 4-manifold with infinite cyclic fundamental group, revised, Journal of Knot Theory and Its Ramifications, 22 (2013) 1350081 (9 pages).

[14] A. Kawauchi, Knot theory for spatial graphs attached to a surface, Proceedings of the ICTS Program: Knot Theory and its Applications, Contemporary Mathematics (to appear).

[15] A. Kawauchi, T. Shibuya and S. Suzuki, Descriptions on surfaces in four-space, I : Normal forms, Math. Sem. Notes, Kobe Univ. 10 (1982), 75-125.

[16] A. Kawauchi, T. Shibuya and S. Suzuki, Descriptions on surfaces in four-space, II: Singularities and cross-sectional links, Math. Sem. Notes, Kobe Univ. 11 (1983), 31-69.

[17] Y. Marumoto, Stable equivalence of ribbon presentations, J. Knot Theory Ramifications, 1 (1992), 241-251.

[18] W. Magnus, A. Karrass and D. Solitar, Combinatorial group theory, Interscience Publishers (1966).

[19] Y. Nakanishi, On ribbon knots, II, Kobe J. Math. 7 (1990), 199-211.

[20] C. Rourke, What is a welded link ?, Intelligence of Low Dimensional Topology 2006, (2007), 263-270, World Sci. Publ. Co..

[21] S. Satoh, Virtual knot presentation of ribbon torus-knots, J. Knot Theory Ramifications, 9 (2000), 531- 542.

[22] B. Winter, On codimension two ribbon embeddings, arXiv:0904.0684 (2009).

[23] T. Yajima, On the fundamental groups of knotted 2-manifolds in the 4-space, J. Math. Osaka City Univ., 13 (1962), 63-71.

[24] T. Yajima, On simply knotted spheres in R_4, Osaka J. Math., 1 (1964), 133-152.

[25] T. Yajima, The review article of T. Yanagawa's paper [27], Amer. Math. Soc. Mathematical Reviews (MathSciNet), MR0270360 (42#5249).

[26] T. Yanagawa, On ribbon 2-knots; the 3-manifold bounded by the 2-knot, Osaka J. Math., 6 (1969), 447-164.

[27] T. Yanagawa, On ribbon 2-knots. III. On the unknotting ribbon 2-knots in S^4, Osaka J. Math., 7 (1970), 165-172.